ELEMENTARY STUDY FOR THE EFFECT OF HHC AND ACTIVE FLAP ON BLADE VORTEX INTERACTION

Noboru Kobiki , Akihiko Tsuchihashi ,
Atsushi Murashige , Eiichi Yamakawa

ATIC (Advanced Technology Institute of Commuter-Helicopter, Ltd.)
2 Kawasaki-cho, Kakamigahara City, Gifu Pref., 504 Japan

Abstract

This paper presents the experimental results of the effect of HHC and active flap on the BVI ,which is performed by a one-bladed rotor model in order to evaluate the simplified BVI avoiding the complicated aerodynamic interference caused by a multi-bladed rotor.

The blade surface pressure distribution by pressure transducers, the miss distance between blade and tip vortex by flow visualization and the sound pressure are measured on BVI conditions with and without HHC/Active Flap.

The blade/vortex miss distance obtained on BVI conditions with and without HHC by LLS is compared with the characteristics of pressure measurement and with CAMRAD II analysis. The good correlation among the blade surface pressure, the blade/vortex miss distance and the sound pressure are obtained on BVI conditions.

The efficiency to alleviate BVI phenomena is compared between HHC and the active flap. It is indicated by the wind tunnel testing that the active flap needs less drive torque to generate the same BVI relief effect as HHC does.

Notation

Symbols

r	Blade spanwise station
R	Rotor radius =1m
μ	Advance ratio
ψ	Rotor azimuth angle (deg.)
ψ_{HHC}, ψ_{AF}	HHC/Active Flap phase angle (deg.) which is defined as the rotor azimuth angle where the blade pitch angle or the active flap deflection becomes their minimum as below.

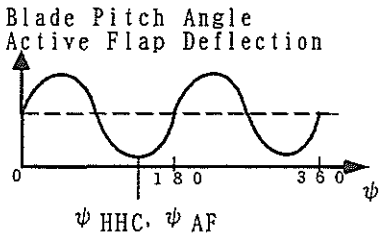

V_W	Wind tunnel speed (m/sec)
x/c	Ratio of the distance from the blade leading edge to the blade chord length(%)
C_p	Pressure coefficient
ΔC_{pmax}	Pressure fluctuation index

Abbreviations/Subscripts

AF	Active Flap
BVI	Blade Vortex Interaction
HHC	Higher Harmonic Control
LLS	Laser Light Sheet

Introduction

BVI noise is generated during the flight condition when a helicopter approaches to the landing area and this noise has the frequency band around 500 to 1,500 Hz which causes significant annoyance to the sense of hearing.

In order to improve this BVI noise problem, especially in the neighbor of heliports, many research programs have been carried out briskly for these decades. For examples, a large scale international cooperative research performed by five organizations from four countries (Refs.1,2,3 and 4) and a fundamental study to focus on understanding BVI phenomena (Refs.5,6,7 and 8).

BVI is generated by the aerodynamic interference between the tip vortex coming out of the preceding blade and the following blade itself, which causes abrupt change of the surface pressure on the following blade, then generates the impulsive BVI noise. The governing factors of BVI are the blade/vortex miss distance, the lift of the interfered blade and the strength of the shed tip vortex.

The mechanism to reduce the BVI noise by HHC is to favorably change these factors by superposing the higher frequency blade pitch change with the proper combination of the frequency, amplitude and phase angle with respect to the rotor azimuth on the conventional collective and 1/rev cyclic pitch change. The demerit of HHC in the practical use is its necessity of the high powered dynamic actuators to drive the whole blades from the root to tip against the high inertia load caused by the high frequency blade pitch change.

Recently, the active flap concept was introduced as a new technology for BVI noise reduction and its capability was demonstrated by a wind tunnel testing. (Refs.9 and 10) Because the active flap is a small trailing edge flap installed in the blade tip region, it is intuitively predicted that the inertia load of the active flap to be overcome by a drive mechanism is much less than that of HHC.

This paper presents the experimental results of BVI phenomenon and HHC/active flap effects on the BVI performed by a one-bladed rotor model which can evaluate the simplified BVI avoiding the complicated aerodynamic interference caused by a multi-bladed rotor. With a modification, both the HHC and active flap configurations can be operated by the same rotor model.

Objectives

In order to avoid the complicated aerodynamic interference caused by a multi-bladed rotor as shown in Fig.1(Ref.3), this work is performed by a one-bladed rotor to study the simplified self-generated BVI as shown in Fig.2 and to evaluate the effects of the HHC and the active flap on BVI.

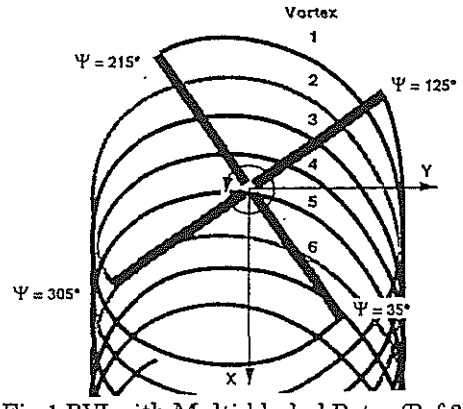

Fig.1 BVI with Multi-bladed Rotor (Ref.3)

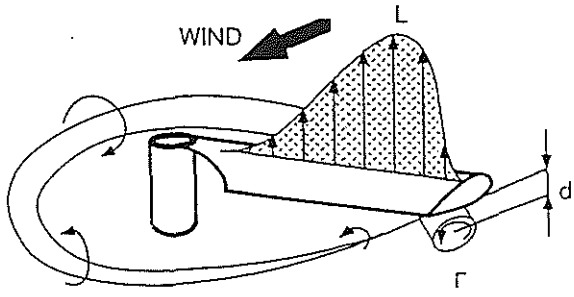

Fig.2 Simplified BVI with One-bladed Rotor

The qualitative degree of the BVI is known to satisfy the relationship as follows (Ref.11);

$$BVI \propto \frac{\Gamma \times L}{d^2} \qquad (1)$$

where

Γ : Vortex strength
L : Blade lift
d : Blade/vortex miss distance

Based on this physical characteristics of BVI, the objectives of this work are focused to study the blade surface pressure, the blade/vortex miss distance and the sound pressure for the evaluation of HHC and the active flap effects on BVI as follows;

1. Elementary, but comprehensive understanding of BVI phenomenon by the measurements of unsteady blade surface pressure, sound pressure and blade/vortex miss distance
2. Evaluation for HHC and active flap effects on BVI by these measurements
3. Efficiency comparison between HHC and active flap
4. Evaluation for the analytical code (CAMRAD II) validity.

Wind Tunnel Testing

Rotor Model

The wind tunnel testings were performed in the two steps. One is done in HHC configuration and the other in the active flap configuration described as follows. The hubs and the blades of both the configurations are rigid for evading aeroelastic influences.

(1)Rotor Model for HHC

The one-bladed model rotor system in HHC configuration is shown in Fig.3 and its primary feature is described in Table 1.

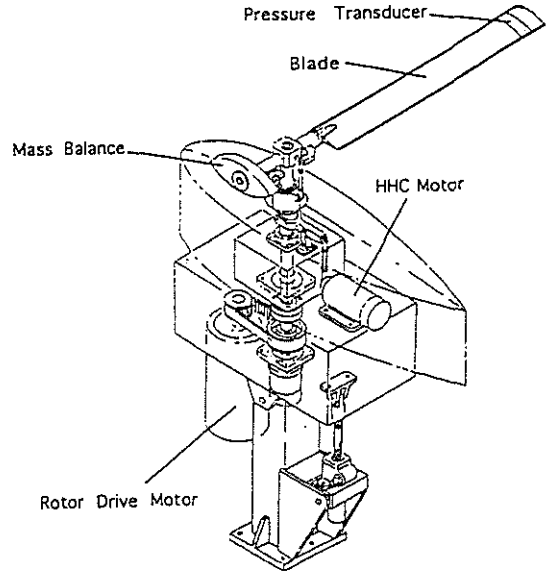

Fig.3 Rotor Model for HHC

Table1 Primary Feature of Rotor Model for HHC

Hub type	rigid in flap and lead-lag
Rotor radius	1m
Blade chord	0.12m
Airfoil	NACA0012
Blade plan form	Rectangular
Rotor rpm	1200rpm (max)
Collective pitch	-5 to +15deg.
Cyclic pitch	-15 to +15deg.
HHC	Amp. : 3deg.(max)
	Freq. : 20Hz (max)
	Phase : variable
Pressure transducer	21 locations at r/R=85%
Tip vortex visualization is available by tracer emission from the blade tip.	

The rotor is driven by the electric motor and the HHC mechanism is driven by the separate electric motor. These two motors are synchronized electrically by the encoder installed in each motor in order to make the proper HHC phase angle shifting with respect to the rotor azimuth angle.

The vertically reciprocating movement of the swash plate for HHC is generated by the lever and crank mechanism which is driven by the eccentric disk installed on the output shaft of the HHC motor. This vertical movement is transmitted to the blade root via. the pitch link and superposed on the conventional collective and cyclic pitch angles.

The combined blade pitch angle (collective + cyclic + HHC) is measured by the potentiometer installed in the rotor hub.

(2)Rotor Model for Active Flap

The one-bladed model rotor system in the active flap configuration is shown in Fig.4 and its primary feature is shown in Table 2.

This configuration is modified from the HHC configuration. The vertically reciprocating movement of the swash plate is generated in the same way as the HHC configuration. This movement is transmitted to the pitch link which makes the rotary reciprocation of the torque tube via. the crank arm and the active flap installed on the other end of the torque tube is oscillated.

Because of the modification, the cyclic pitch can not be changed in the active flap configuration and is fixed to zero. The collective pitch angle is pre-set by the collective fitting which connect the blade and the hub. The collective pitch angle is measured by the same potentiometer as HHC configuration and the active flap deflection by the Hall sensor installed in the mid span of the active flap.

Data Acquisition/Processing

The schematics of the data acquisition and processing system is shown in Fig.5. This system consists of the following three measuring subsystems

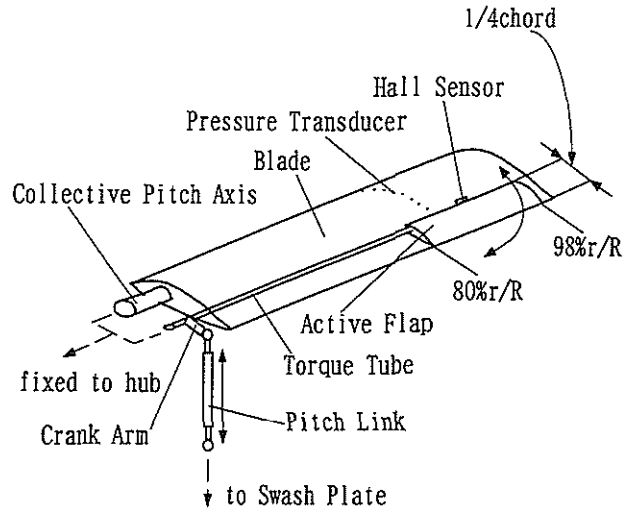

Fig.4 Rotor Model for Active Flap

Table2 Primary Feature of Rotor Model for Active Flap

Hub type	rigid in flap and lead-lag
Rotor radius	1m
Blade chord	0.12m
Airfoil	NACA0012
Blade plan form	Rectangular
Rotor rpm	1200rpm (max)
Collective pitch	-5 to +15deg.
Cyclic pitch	0deg. (fixed)
Active Flap	Amp. : 30deg.(max)
	Freq. : 20Hz (max)
	Phase : variable
Pressure transducer	17 locations on the blade side at r/R=85%
Tip vortex visualization is available by tracer emission from the blade tip.	

and the data processing part.

(1)Blade Surface Pressure

The raw signals coming out from the pressure transducers in the blade are amplified by the pre-amplifier installed on the rotating frame in order to enhance the S/N ratio avoiding the contamination such as EMI. These amplified signals are transferred to the non-rotating frame via. the slip ring. The sampling rate of the blade surface pressure is 6.4kH which is equivalent to 0.56deg. resolution of the rotor azimuth angle under the test condition(rotor rpm=600).

The 1/rev pulse signal generated by the rotary encoder is also acquired simultaneously to correspond the pressure data with respect to the blade azimuth angle.

(2)Flow Visualization for Tip Vortex

The blade tip vortex is visualized by LLS and the tracer is emitted from the blade tip or the dispenser set in upstream side of the rotor system.

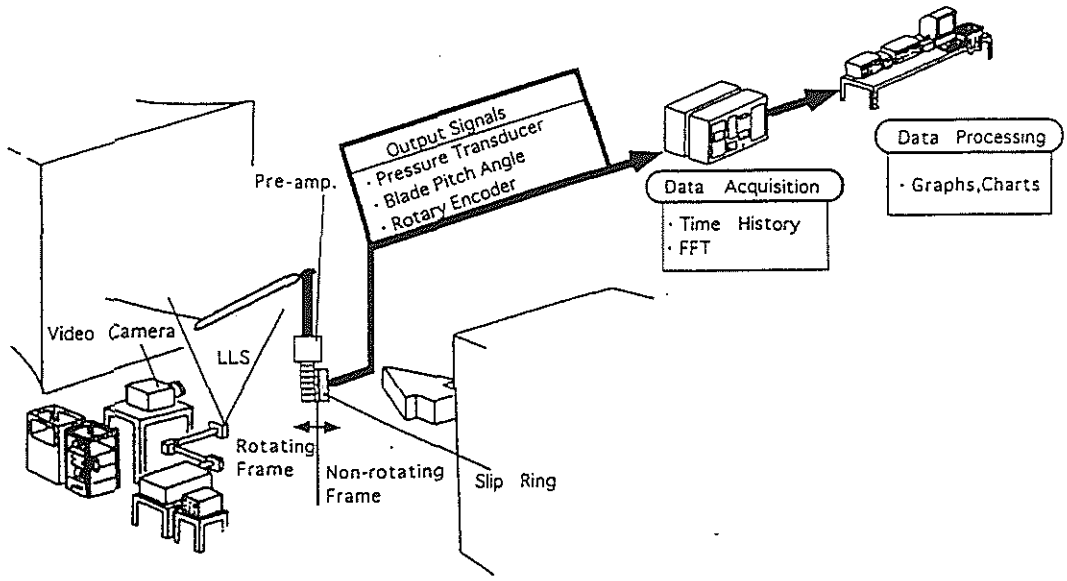

Fig. 5 Data Acquisition/Processing System

The blade/vortex miss distance is obtained by the video camera image analysis.

The LLS is projected vertically from the wind tunnel floor as shown in Fig.5 and Fig.6 so that the 85%r/R blade portion is illuminated at =42deg. where BVI can be clearly seen on the selected test conditions described later and the pressure transducers are located. This choice of the LLS location makes it possible to evaluate the correlation between the blade surface pressure and the blade/vortex miss distance.

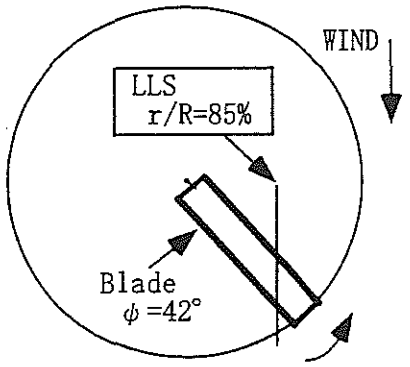

TOP VIEW

Fig.6 LLS Arrangement

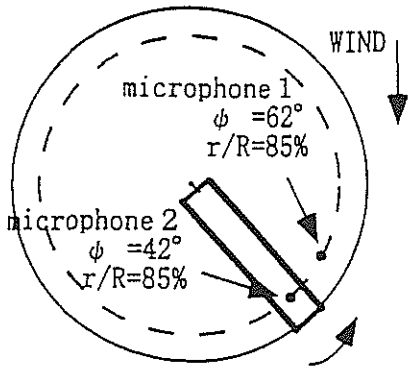

TOP VIEW

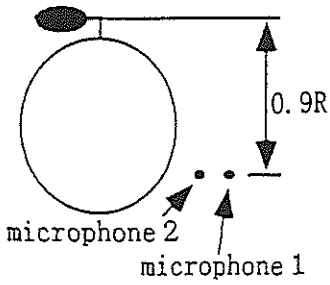

REAR VIEW

Fig.7 Microphone Arrangement

(3)Sound Pressure

The two microphones are set 0.9m below the rotor plane as shown in Fig.7. MIC1 is used to evaluate BVI with and without HHC/Active Flap because this microphone is located at ψ where BVI occurs and at r/R=85% where the pressure transducers are installed, which makes it possible to evaluate the correlation between blade surface pressure characteristics and sound pressure.

(4)Data Processing

The blade surface pressure and the sound pressure which are collected in the time domain are ensemble averaged over 30 rotor revolutions in order to eliminate the random noise and to make the periodical aeroacoustic variation caused by the rotor revolution clear.

Test Condition

The wind tunnel testing was conducted in 2.5× 2.5m Low Speed Wind Tunnel of Kawasaki Heavy Industries, Ltd. on the test conditions as below.

Wind tunnel speed	20.1m/sec
Test section	open jet, not anechoic
Rotor rpm	600rpm
Blade pitch angle	
collective	5deg.
cyclic	0deg.
Rotor shaft angle	0deg.
HHC	
frequency	2/rev (20Hz)
amplitude	2deg.
phase angle	variable
Active Flap	
frequency	2/rev (20Hz)
amplitude	6, 18 and 24deg.
phase angle	variable

The combination of the wind tunnel speed and the rotor rpm is obtained by CAMRAD II so that BVI occurs as parallel as possible within the performance envelope of the rotor system .

Experimental Results

HHC

The blade pressure at x/c=2.15%, r/R=85% on the upper surface with respect to the rotor azimuth with and without HHC (2/rev, 2 deg. amplitude) is shown in Fig.8. The effective angle of attack of the blade segment is being decreased by the approach of the tip vortex to the blade and vice versa, which makes the abrupt pressure change. Fig.8 clearly shows this BVI phenomenon captured as this abrupt pressure change process in a short time period at around ψ=42deg.

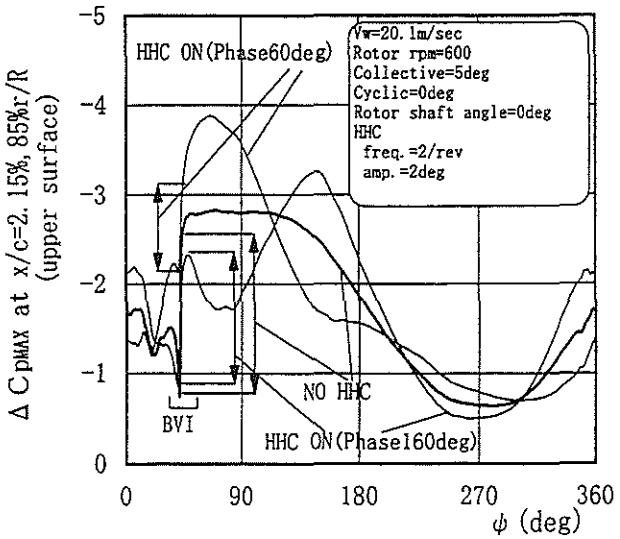

Fig.8 Blade Surface Pressure Characteristics

Fig.8 also shows the effect of the HHC application on the degree of BVI. The magnitude of C_p gap at the BVI region has the difference between HHC on and off. In this case, ψ_{HHC} =60 and 160deg. have the large BVI relief effect. In order to evaluate this BVI relief effect, the pressure fluctuation index which physically means the maximum value of the deference in the pressure coefficient between the successive ψ's is introduced and defined as below.

$$PressureFluctuationIndex: \Delta C_{p\max} = \max(\Delta C_p(\psi_i)) \quad (2)$$

$$\Delta C_p(\psi_i) = C_p(\psi_i) - C_p(\psi_{i-1})$$

$$\psi_i - \psi_{i-1} = 0.56\text{deg.}$$

$$C_p = \frac{P - P_s}{q}$$

where

P : measured pressure

P_s : static pressure

q :dynamic pressure at 85%r/R as Vw=0m/sec

ΔC_{pmax} is always obtained at ψ where the BVI takes place.

Fig.9 shows the blade surface pressure characteristics reduced in Δ Cp over the interested ψ range around BVI.

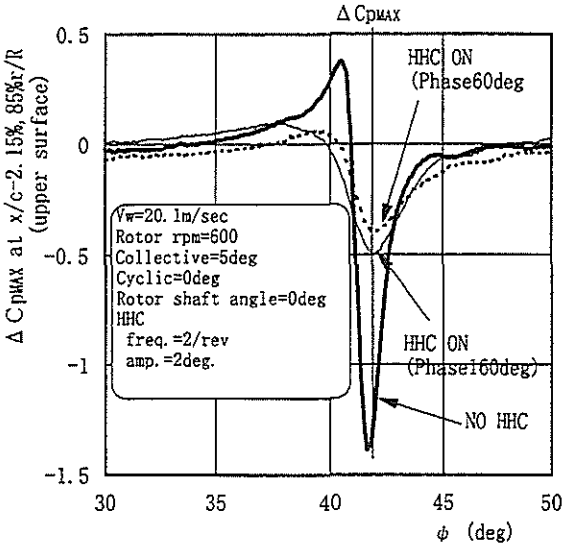

Fig.9 Blade Surface Pressure Fluctuation Characteristics

ΔC_{pmax} of ψ_{HHC}=60 and 160deg. cases are reduced to 35% of HHC off case. It is noted that ΔC_p of HHC off case largely changes in the positive direction in the beginning of the BVI (ψ=41deg.) as well as in the negative direction in the middle of the BVI (ψ =42deg.).

More systematic study for the effect of HHC phase angle on ΔC_{pmax} is shown in Fig.10 and the corresponding effect on the blade/vortex miss distance is shown in Fig.11.

The minimum absolute value of ΔC_{pmax} is obtained at ψ_{HHC}=60 and 160deg in case of 2/rev HHC application, which means the maximum BVI relief effect is attained at these ψ_{HHC}'s. The opposite happens at ψ_{HHC}=20 and 100deg.

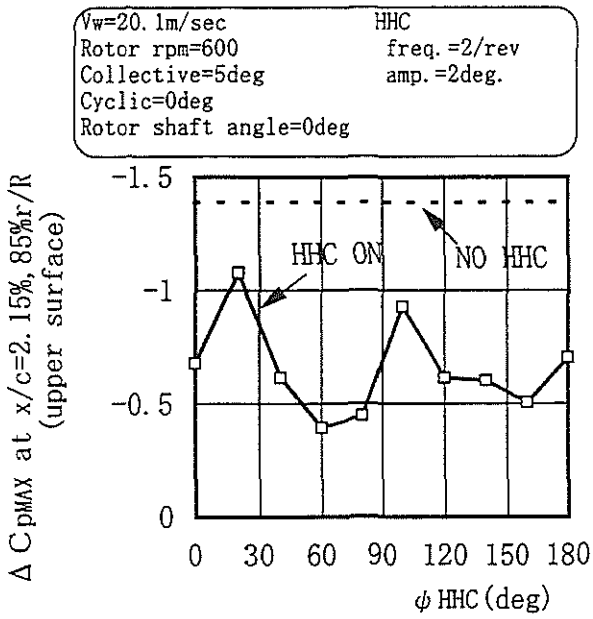

Fig.10 Effect of ϕ_{HHC} on Blade Surface Pressure

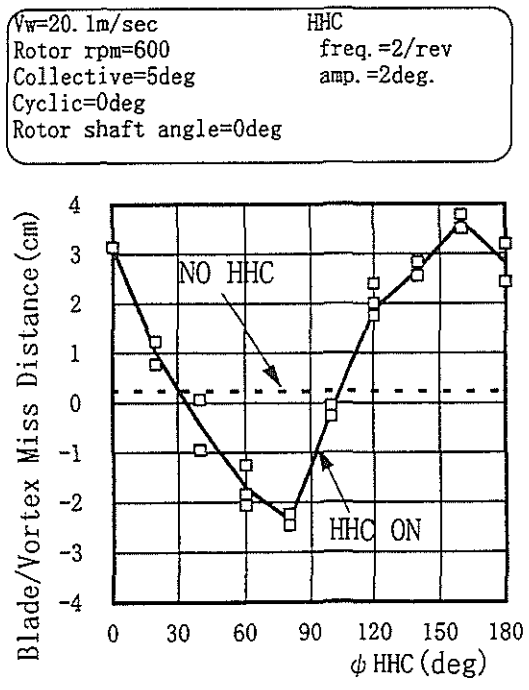

Fig.11 Effect of ϕ_{HHC} on Blade/Vortex Miss Distance

The maximum blade/vortex miss distance is obtained at ϕ_{HHC}=80 and 160deg. The tip vortex passes most downward the blade in the former case and most upward in the latter case, which is observed by LLS and described later. When HHC is not applied, the blade/vortex miss distance is nearly zero meaning the head-on collision between the blade and the tip vortex. This also takes place in HHC on cases at about ϕ_{HHC}=30 and 100deg. estimated by interpolating the measured data points on Fig.11.

Studying these two figures together, the negative correlation between ΔC_{pmax} and the blade/vortex miss distance with respect to ϕ_{HHC} is obtained. The most optimum ϕ_{HHC} for the BVI relief makes the blade/vortex miss distance maximum and the absolute value of ΔC_{pmax} minimum simultaneously. The some discrepancy in ϕ_{HHC} between ΔC_{pmax} and the blade/vortex miss distance which makes the largest BVI relief effect mainly comes from the inadequate number of the measuring points. It is predicted that much more measuring points make the curves in Fig.10 and Fig.11 sinusoidal fairlier and the agreement with respect to ϕ_{HHC} between the two curves better.

The correlation among the blade surface pressure distribution, the blade local lift, the blade/vortex miss distance and the sound pressure at the moment of BVI is shown in Fig.12(a) through (d).

The pressure distribution shown in Fig.12(a) shows the difference in the degree of BVI clearly in both cases of HHC on(ϕ_{HHC}=60 and 160deg.) and HHC off. The cases of ϕ_{HHC}=60 and 160deg. are selected because these two ϕ_{HHC}'s have the maximum blade/vortex miss distance but have the tip vortex passing on the opposite side of the blade as shown in Fig.12(c). It is also shown in Fig.12(a) that C_p in the less than 25% x/c region of the HHC off case changes largely between ϕ = 41 deg. and 43 deg. where the BVI takes place. On the other hand, these of HHC on cases have much smaller C_p change in this region of ϕ.

The sharp change in the blade local lift at 85%r/R which is obtained by the integration of the pressure distribution over the blade occurs at about ϕ = 42 deg. for both HHC on and off cases as shown in Fig.12(b). But this change for HHC on cases is about a half of that for HHC off case.

It is well explained by investigation of the chordwise pressure distribution immediately before(ϕ = 41 deg.) and after(ϕ = 43 deg.) the rotor azimuth angle where BVI takes place. For HHC on cases, the change of the surface pressure peak near the blade leading edge in the direction to increase the local lift caused by the tip vortex approach is smaller than that for HHC off case.

Fig.12 (c) shows the relative spatial relationship between the blade and the tip vortex visualized by LLS. Although the HHC off case has the head-on collision, the blade and the tip vortex are well apart in HHC on cases of ϕ_{HHC}=60 and 160deg.

The measured sound pressure shown in Fig.12(d) also indicates the effect of HHC on the BVI noise reduction consistently to the pressure data and the flow visualization. It is noted that even the ϕ_{HHC}=60deg. case has the larger local lift than the HHC off case around the rotor azimuth angle range where BVI takes place, but has the smaller BVI noise. This implies that among the three factors governing the BVI shown in Eq.(1), the blade lift has the less effect on BVI than the vortex strength and the blade/vortex miss distance.

As a result, the larger blade/vortex miss distance makes the smaller pressure change, which makes BVI noise reduction.

Vw=20.1m/sec　　Collective=5deg.
Rotor rpm=600　　Cyclic=0deg.
Rotor shaft angle=0deg

NO HHC

HHC ON
freq.=2/rev.amp.=2deg..phase=60deg.

HHC ON
freq.=2/rev.amp.=2deg..phase=160deg

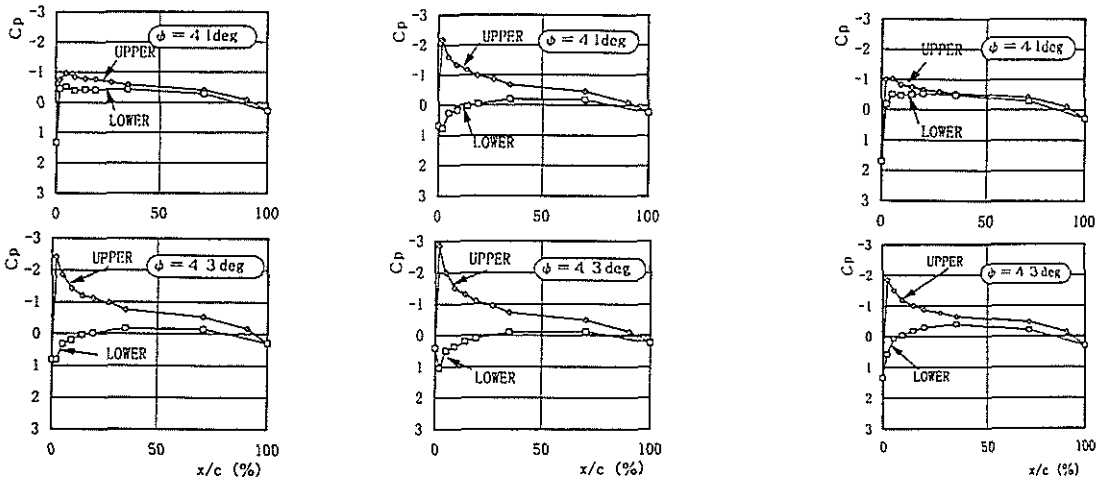

(a) Pressure Distribution at x/c=2.15%,85%r/R (upper surface)

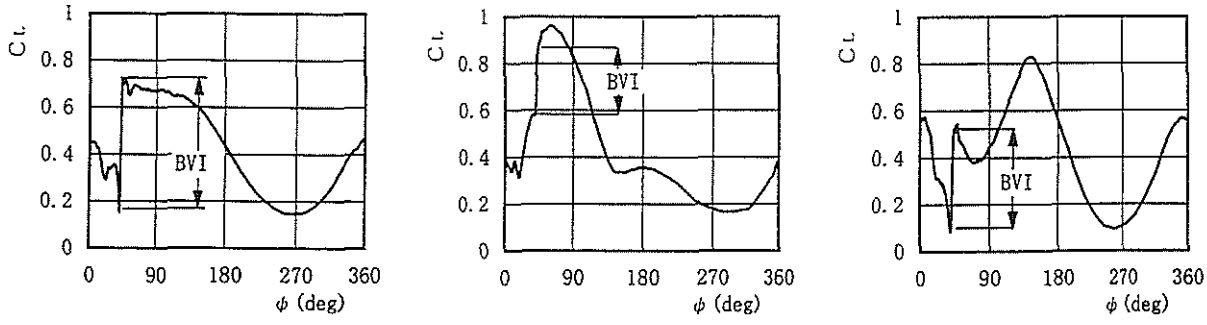

(b) Blade Local Lift at 85%r/R

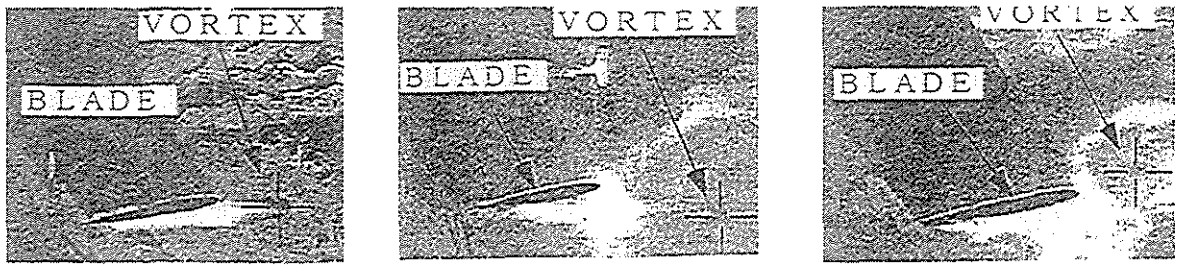

(c) LLS

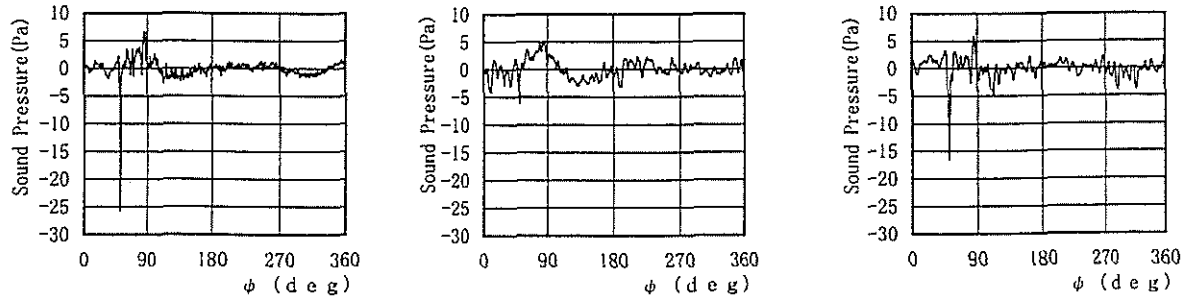

(d) Sound Pressure

Fig.12 Comprehensive Comparison of BVI Measurement

Active Flap

The 2/rev active flap effect is studied by the wind tunnel testing. Δ Cp_{max} at x/c=2.15% on the upper surface of the blade with respect to the active flap phase angle is shown in Fig.13 at the active flap amplitude of 6, 18 and 24deg. The corresponding blade/vortex miss distance obtained by the 2/rev active flap is shown in Fig.14. at the active flap amplitude of 6 and 24deg. The missing data points at the active flap amplitude of 24deg. in Fig.14 are caused by the unclear video image of the tip vortex. The circled portions A through D on the both figures correspond in the same range of the active flap phase angle, which are set for the convenience of quotation.

Fig.15 shows the measured sound pressure with respect to the rotor azimuth at the active flap amplitude of 6 and 24deg. with and without the active flap application. The active flap phase angles in this figure are selected ψ_{AF}=80 and 140deg. to represent the portions C and D, respectively where the active flap has the maximum effect for BVI alleviation.

In the portions A and B, the absolute values of Δ Cp_{max} have their maximum and the blade/vortex miss distances become nearly zero. These two are consistent to indicate that the strong BVI takes place at these active flap phase angles.

In the portions C and D, the opposite to the portions A and B occurs and the BVI is alleviated, which is demonstrated by the measured sound pressure shown in Fig.15.

The larger amplitude of the active flap is applied, the larger BVI relief effect is obtained based on the observation of Fig. 13 through 15. But the pressure data shown in Fig.13 shows that this favorable effect by the increment of the active flap amplitude is maintained up to the active flap amplitude of 18deg. and saturated by the larger than this active flap amplitude.

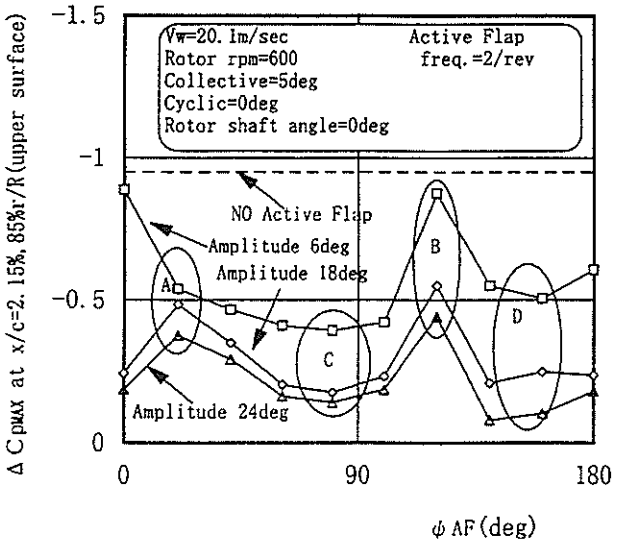

Fig.13 Active Flap Effect on Blade Surface Pressure

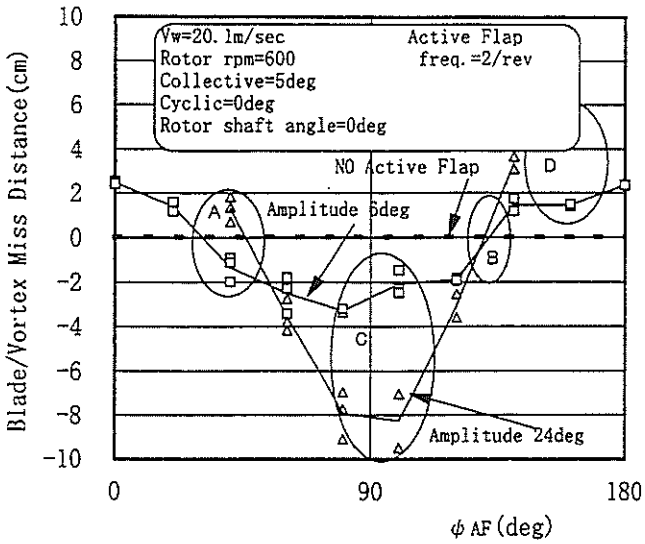

Fig.14 Active Flap Effect on Blade/Vortex Miss Distance

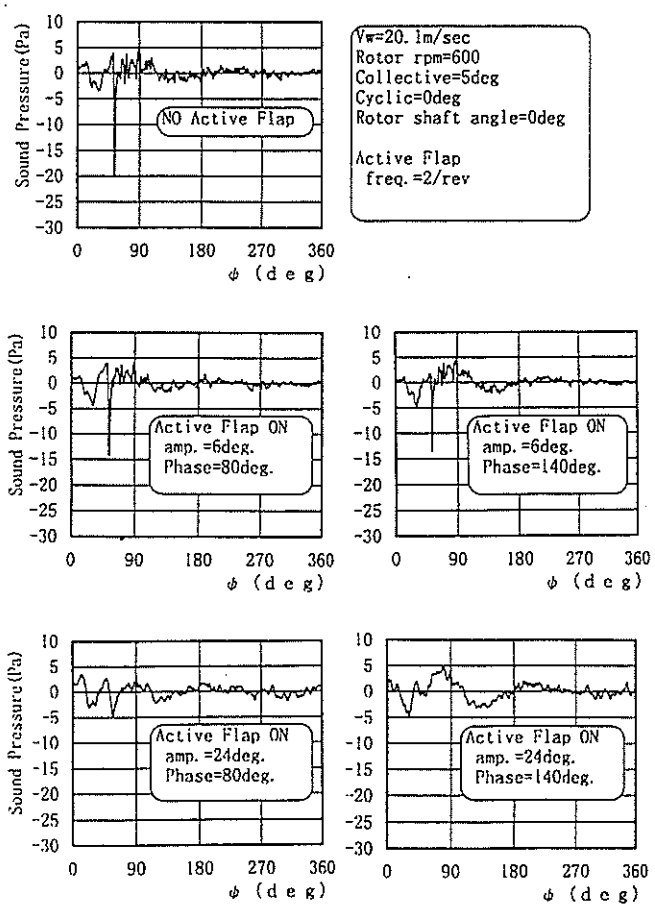

Fig.15 Active Flap Effect on Sound Pressure at BVI

Comparisons between HHC and Active Flap

The comparison of the BVI relief effect between HHC and the active flap is performed with respect to the drive torque required to drive each configuration. The drive torque index is introduced to describe the equivalent driving torque of the HHC and the active flap configurations for this purpose and defined as follows considering the unique components of the rotor system for each configuration.

$$DriveTorqueIndex = \log_{10}\left(\frac{J \bullet \Delta\theta \bullet f^2}{T_o}\right) \qquad (3)$$

$$T_o = J_{AF} \bullet \Delta\theta_o \bullet f_o^2$$

where

J : Inertia moment of the entire blade for HHC configuration (J_{HHC}) or inertia moment of the active flap for the active flap configuration(J_{AF})

$\Delta\theta$: Amplitude of HHC($\Delta\theta_{HHC}$) or active flap($\Delta\theta_{AF}$)

$\Delta\theta_o \equiv 1$deg.

f : Frequency of HHC(f_{HHC}) or active flap(f_{AF})

$f_o \equiv 20$Hz

The comparison of ΔCp_{max} at x/c=2.15% on the upper surface of the blade with respect to the drive torque index is shown in Fig.16. The comparison of the blade/vortex miss distance is shown in Fig.17. The data points on these figures are obtained by several combination of $\Delta\theta$ and f.

The experimental comparisons shown above indicate the followings.

The active flap configuration, which drives a comparatively small flap installed in the blade tip portion, can produce the same degree of ΔCp_{max} more efficiently than the HHC configuration, which drives whole the blade from the blade root.

The active flap configuration can make the same degree of the blade/vortex miss distance more efficiently than the HHC configuration.

Consequently, the active flap configuration is able to alleviate BVI more efficiently than the HHC configuration.

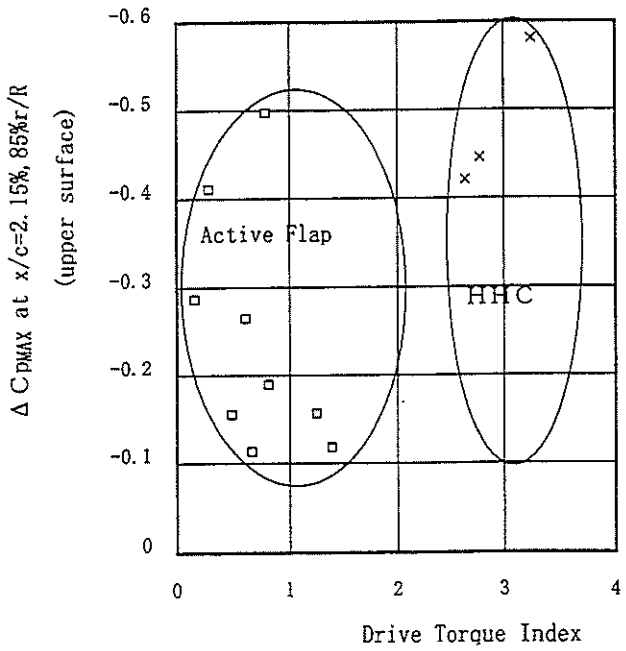

Fig.16 BVI Relief Effect Comparison of ΔCp_{max} between HHC and Active Flap

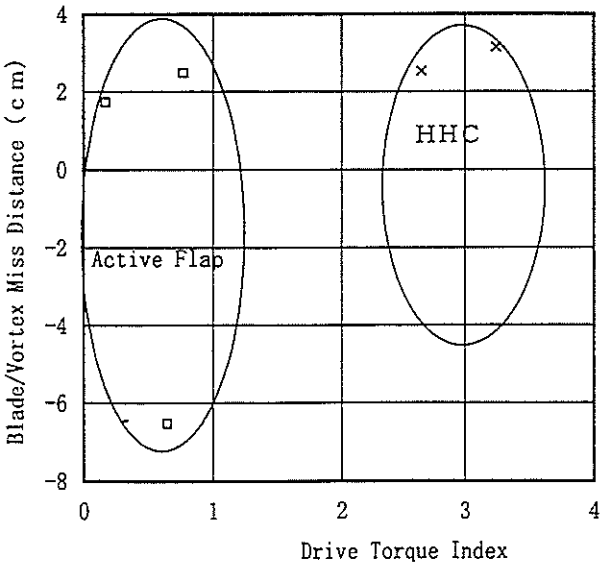

Fig.17 BVI Relief Effect Comparison of Blade/Vortex Miss Distance between HHC and Active Flap

Comparisons between Analysis and Experiment

The blade/vortex miss distances obtained experimentally and analytically in the HHC configuration are shown in Fig.18, because the blade/vortex miss distance is the only quantity with which the experiment and CAMRAD II analysis can be directly compared. The curve of the experimental blade/vortex miss distance is numerically the same one as shown in Fig.11.

Fig.18 shows that although the both have the sinusoidal property with respect to ϕ_{HHC} with the blade/vortex miss distance of the HHC off case as a center value, the experimentally obtained blade/vortex miss distance is 35mm less than and 30deg. in ϕ_{HHC} ahead of that obtained by CAMRAD II.

The reason for the quantitative discrepancy between the two can exist in the wind tunnel flow deflection which is not modeled in the analysis and is believed to have a significant effect on the blade/vortex miss distance.

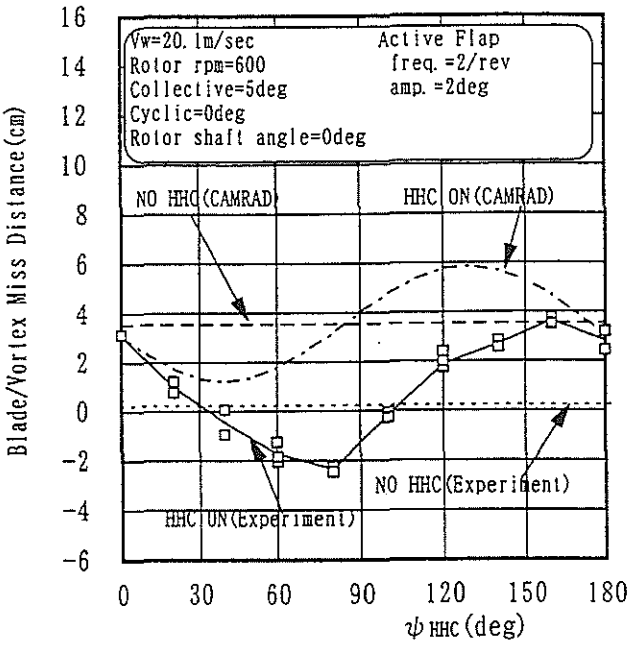

Fig.18 Comparison of Blade/Vortex Miss Distance between Analysis and Experiment

Conclusions

Summarizing the experimental and analytical results, the followings are concluded.

1. BVI phenomena and the effects of HHC and active flap on BVI are quantitatively evaluated by the measurements of the blade surface pressure, the sound pressure and the blade/vortex miss distance. The good correlation among the three are obtained under the conditions with and without HHC/Active Flap.

2. The blade/vortex miss distances obtained by both the experiment and the CAMRAD II analysis have the sinusoidal property with respect to ψ_{HHC} with the blade/vortex miss distance of the HHC off case as a center value, but there is a numerical discrepancy between them. CAMRAD II analysis with a stricter modeling is required.

3. The larger amplitude of the active flap can make the larger BVI relief effect. But it is predicted based on the experimental result that this favorable effect by the increment of the active flap amplitude is maintained up to the active flap amplitude of 18deg. and saturated by the larger than this active flap amplitude.

4. With less drive torque, the active flap can produce the same degree of BVI relief effect as HHC can.

Acknowledgments

The authors wish to express their thanks to Mr. Hakojima and his staff of Japan Aircraft Mfg. Co. Ltd. for their special efforts to design and manufacture the HHC configuration of the rotor system and to Mr. Uchida and his team of Kawasaki Gifu Engineering Co. Ltd. for their redesigning effort from HHC to the active flap configuration. Also our thanks to the crew of Low Speed Wind Tunnel lead by Mr. Isaji and Mr. Yamada of Kawasaki Heavy Industries, Ltd. for their support to perform the elaborate wind tunnel testings and measurement.

References

Conference Proceedings

1. Splettstroesser,W.R., Lehmann, G., v.d. Wall, B., "Initial Result of a Model Rotor Higher Harmonic Control (HHC) Wind Tunnel Experiment on BVI Inpulsive Noise Reduction",15th European Rotorcraft Forum, Amsterdam , The Netherlands, September 1989, Paper 01.

2. Splettstroesser,W.R., Schultz, K-J., Kube , R., Brooks, T.F., Booth, E.R., Niesl, G., Streby, O., "BVI Impulsive Noise Reduction by Higher Harmonic Pitch Control:Results of a Scaled Model Rotor Experiment in the DNW",17th European Rotorcraft Forum, Berlin, Germany, September 1991, Paper 61.

3. Gmelin, B., Heller, H., Philippe, J.J., Mercker, E., Preisser, J.S., "HHC Aeroacoustics Rotor Test at the DNW: The Joint German/French/US HART Project" ,20th European Rotorcraft Forum, Amsterdam, The Netherlands, October 1994, Paper 115.

4. Gmelin, B.L., Heller, H., Mercker, E., Philippe, J.J., Preisser, J.S., Yu, Y.H., "The HART Programme : A Quadrilateral Cooperative Research Effort", 51st Annual Forum of the American Helicopter Society, FortWorth,TX,May 1995, pp 695-709.

5. Kokkalis, A., Galbraith, R.A.McD., " Description of, and Preliminary Results from, a New Blade-Vortex Interaction Test Facility",12th European Rotorcraft Forum, Garmisch-Partenkirchen, Germany, September 1986, Paper 80.

6. Kokkalis, A., Galbraith, R.A.McD., " Results from the Glasgow University Blade/Vortex Interaction(B.V.I.) Facility",13th European Rotorcraft Forum, Arles, France, September 1987, Paper 2.18.

7. Horner, M.B., Saliveros,E., Galbraith, R.A.McD., " An Experimental Investigation of the Oblique Blade-Vortex Interaction",17th European

Rotorcraft and Powered Lift Aircraft Forum, Berlin, Germany, September 1991, pp 483-493.

8. Coton, F.N., de la Iglesia Moreno, F., Galbraith, R.A.McD., Horner, M.B., " A Three -Dimensional Model of Low Speed Blade-Vortex Interaction",20th European Rotorcraft Forum, Amsterdam, The Netherlands, October 1994, Paper 18.

9. Dawson, S., Marcolini, M., Booth, E., Straub, F., Hassan, A., Tadghighi, H., Kelly, H., " Wind Tunnel Test of an Active Flap Rotor: BVI Noise and Vibration Reduction", 51st Annual Forum of the American Helicopter Society, FortWorth,TX,May 1995, pp 631-648.

10. Straub, F., " Active Flap Control for Vibration Reduction and Performance Improvement", 51st Annual Forum of the American Helicopter Society, FortWorth,TX,May 1995, pp 381-392.

Periodical Articles

11. Hardin, J.C., Lamkin, S.L., " Concepts for Reduction of Blade/Vortex Interaction Noise", Journal of Aircraft Vol.24,No.2, pp 120-125.